J|A|C|S
ARTICLES
Published on Web 12/02/2003

Polymerization from the Surface of Single-Walled Carbon Nanotubes − Preparation and Characterization of Nanocomposites

Zhaoling Yao,[†] Nadi Braidy,[‡] Gianluigi A. Botton,[‡] and Alex Adronov*,[†]

Contribution from the Departments of Chemistry, Materials Science and Engineering, and the Brockhouse Institute for Materials Research (BIMR), McMaster University, Hamilton, Ontario L8S 4M1, Canada

Received July 27, 2003; E-mail: adronov@mcmaster.ca

Abstract: Single-walled carbon nanotubes were functionalized along their sidewalls with phenol groups using the 1,3-dipolar cycloaddition reaction. These phenols could be further derivatized with 2-bromoisobutyryl bromide, resulting in the attachment of atom transfer radical polymerization initiators to the sidewalls of the nanotubes. These initiators were found to be active in the polymerization of methyl methacrylate and *tert*-butyl acrylate from the surface of the nanotubes. However, the polymerizations were not controlled, leading to the production of high molecular weight polymers with relatively large polydispersities. The resulting polymerized nanotubes were analyzed by IR, Raman spectroscopy, DSC, TEM, and AFM. The nanotubes functionalized with poly(methyl methacrylate) were found to be insoluble, while those functionalized with poly(*tert*-butyl acrylate) were soluble in a variety of organic solvents. The *tert*-butyl groups of these appended polymers could also be removed to produce nanotubes functionalized with poly(acrylic acid), resulting in structures that are soluble in aqueous solutions.

Introduction

The potential utility of single-walled carbon nanotubes (SWNTs)[1] in a variety of technologically important applications, such as molecular wires and electronics,[2,3] sensors,[4] high-strength fibers,[5] and field emission,[6] is now well established. The conductivity and tensile strength[7] properties of this new class of nanoscale materials have attracted a great deal of investigation, which has immensely expanded their scope of applicability. For example, the recent work of Dekker,[8−10] Lieber,[11−14] and Avouris[2] has demonstrated that SWNTs can not only be utilized as the semiconducting channels in functional field effect transistors (FETs), but that they can also outperform comparable Si-based devices. In addition, Dai and co-workers have shown that SWNTs can act as chemical sensors, where exposure to specific gases, including NH_3, NO_2, and H_2, alters nanotube conductivity by up to 3 orders of magnitude within several seconds of exposure.[15,16] However, despite this significant research progress, several major limitations have yet to be overcome and currently preclude the widespread commercial utility of carbon nanotubes. Among these, the inherent insolubility of SWNTs in most organic and aqueous solvents is a limiting factor that must be overcome if carbon nanotubes are to be utilized within widespread applications such as the preparation of blends with conventional polymers, molecular electronics, and the production of homogeneously dispersed conducting layers within electroluminescent devices.

Recently, a number of research groups have focused on the functionalization of carbon nanotubes, and especially SWNTs with various organic, inorganic, and organometallic structures using both covalent and noncovalent approaches.[17] The primary focus of many of these studies has concentrated on improving the solubility properties of nanotubes. Initial success was achieved by functionalizing carboxylic acid groups, formed at the ends and defect sites of SWNTs during oxidative purification/shortening,[18,19] through amidation with alkylamines such as octadecylamine. Over the past five years, this approach has

[†] Department of Chemistry.
[‡] Department of Materials Science and Engineering.

(1) Iijima, S.; Ichihashi, T. *Nature* **1993**, *363*, 603−605.
(2) Avouris, P. *Acc. Chem. Res.* **2002**, *35*, 1026−1034.
(3) Collins, P. G.; Avouris, P. *Sci. Am.* **2000**, *283*, 62−69.
(4) Dai, H. J. *Acc. Chem. Res.* **2002**, *35*, 1035−1044.
(5) Ajayan, P. M. *Chem. Rev.* **1999**, *99*, 1787−1799.
(6) Choi, W. B.; Chung, D. S.; Kang, J. H.; Kim, H. Y.; Jin, Y. W.; Han, I. T.; Lee, Y. H.; Jung, J. E.; Lee, N. S.; Park, G. S.; Kim, J. M. *Appl. Phys. Lett.* **1999**, *75*, 3129−3131.
(7) Yu, M.-F.; Files, B. S.; Arepalli, S.; Ruoff, R. S. *Phys. Rev. Lett.* **2000**, *84*, 5552−5555.
(8) Bachtold, A.; Hadley, P.; Nakanishi, T.; Dekker, C. *Science* **2001**, *294*, 1317−1320.
(9) Postma, H. W. C.; Teepen, T.; Yao, Z.; Grifoni, M.; Dekker, C. *Science* **2001**, *293*, 76−79.
(10) Yao, Z.; Dekker, C.; Avouris, P. *Carbon Nanotubes*; Springer: New York, 2001; Vol. 80, pp 147−171.
(11) Duan, X. F.; Huang, Y.; Lieber, C. M. *Nano Lett.* **2002**, *2*, 487−490.
(12) Ouyang, M.; Huang, J. L.; Lieber, C. M. *Acc. Chem. Res.* **2002**, *35*, 1018−1025.
(13) Ouyang, M.; Huang, J. L.; Cheung, C. L.; Lieber, C. M. *Science* **2001**, *291*, 97−100.
(14) Rueckes, T.; Kim, K.; Joselevich, E.; Tseng, G. Y.; Cheung, C. L.; Lieber, C. M. *Science* **2000**, *289*, 94−97.
(15) Kong, J.; Franklin, N. R.; Zhou, C. W.; Chapline, M. G.; Peng, S.; Cho, K. J.; Dai, H. J. *Science* **2000**, *287*, 622−625.
(16) Kong, J.; Chapline, M. G.; Dai, H. J. *Adv. Mater.* **2001**, *13*, 1384−1386.
(17) Hirsch, A. *Angew. Chem., Int. Ed.* **2002**, *41*, 1853−1859.
(18) Liu, J.; Rinzler, A. G.; Dai, H. J.; Hafner, J. H.; Bradley, R. K.; Boul, P. J.; Lu, A.; Iverson, T.; Shelimov, K.; Huffman, C. B.; Rodriguez-Macias, F.; Shon, Y. S.; Lee, T. R.; Colbert, D. T.; Smalley, R. E. *Science* **1998**, *280*, 1253−1256.

been extended to the attachment of organometallic complexes, including Vaska's complex[20] and Wilkinson's catalyst,[21] inorganic nanocrystals such as CdSe[22,23] and Au,[24] DNA,[25,26] and various other biological molecules,[27−30] dendrons,[31] and polymers.[32]

Another strategy for SWNT functionalization involves the use of sidewall reactions such as fluorination with elemental fluorine,[33] 1,3-dipolar cycloaddition,[34,35] electrochemical reduction of diazonium salts,[36] and direct addition of nitrenes, carbenes, and radicals to the unsaturated π-system of the nanotubes.[37] These covalent functionalization strategies have opened up a wide range of chemistry that can be performed on the sidewalls of carbon nanotubes, allowing chemists to control the properties of these nanoscale materials. Additionally, a number of recent reports have concentrated on supramolecular functionalization of SWNTs, especially with polymeric structures. The aromatic sidewalls of nanotubes provide the possibility for π-stacking interactions with conjugated polymers[38−43] as well as polycyclic aromatic hydrocarbons. The use of substituted pyrene molecules for surface attachment of a number of functionalities has also been implemented, where the appended structure has been used to attach proteins,[44] polymerization initiators,[45] or aqueous solubilizing groups[46] in a noncovalent fashion.

With the goal of improving the solubility properties of carbon nanotubes kept in mind, it is reasonable to assume that attachment of large, soluble molecules to carbon nanotubes in either a covalent or a noncovalent manner should have the largest impact on solubility. Indeed, this has been the impetus for functionalization of nanotubes with dendrons and polymers.[31,32] However, until now, covalent attachment of polymers to carbon nanotubes has been mainly accomplished using a "grafting to" approach, in which the polymer is first prepared and then reacted with the carboxylic acid functionalities of the SWNTs. Here, we describe a "grafting from" approach to the "growth" of polymers from the surface of nanotubes by first covalently attaching polymerization initiators and then exposing the nanotube-based macroinitiators to monomers. Because this approach strictly involves the reaction of the nanotubes with small molecules, it was expected that a higher incorporation of polymers would result relative to the "grafting to" approach. In addition, this approach is highly modular, allowing for the preparation of nanotube-based macroinitiators that can be used to polymerize a wide range of monomers. We have chosen to investigate the use of atom transfer radical polymerization (ATRP),[47] which has been shown to be a highly versatile technique for the controlled radical polymerization of acrylate-based monomers from the surface of nanoscale structures.[48,49]

Results and Discussion

Nanotube Shortening. The carbon nanotube starting materials we utilized were approximately 1.5−2 μm in length, and 1−1.5 nm in diameter. Because our primary goal for polymer-functionalized nanotubes was enhanced solubility, we postulated that functionalization of shortened nanotubes would have a higher probability of producing soluble structures. The shortening procedure we followed was a slightly modified version of the procedure published by Smalley and co-workers.[18] Our only modification was a reduced sonication time in the 3:1 mixture of H_2SO_4:HNO_3 from 24 h to approximately 3 h. In our hands, and with our ultrasonicator (Branson Ultrasonics B1510), it was found that sonication for more than 6 h leaves no trace of carbon nanotubes, as determined by atomic force microscopy (AFM). This may be due to a difference in sonicating power between the Branson (70 W) sonicator we used and the Cole Parmer (20 W) sonicator used by Smalley. Figure 1 shows AFM images of carbon nanotubes at different sonication time periods. It is clear that a substantial length decrease is occurring after only a short period of sonication. It should be noted that the purchased nanotube samples are polydisperse in terms of length, and, therefore, a variety of different lengths can be observed in each AFM image. Length analysis of 100 different nanotubes after 2 h of shortening indicated an average length of 334 ± 123 nm. The shortened SWNTs were isolated by filtration through a polycarbonate membrane having a pore size of 100 nm. The product of this procedure was characterized by IR spectroscopy and exhibited the expected C═O stretch at 1741 cm^{-1} arising from the carboxylic acid groups introduced as a result of the shortening process (Figure 2A).[19,50] The large IR band observed at ca. 3400 cm^{-1} and the weak one at 1627 cm^{-1} are attributed

(19) Chen, J.; Hamon, M. A.; Hu, H.; Chen, Y.; Rao, A. M.; Eklund, P. C.; Haddon, R. C. *Science* **1998**, *282*, 95−98.
(20) Banerjee, S.; Wong, S. S. *Nano Lett.* **2002**, *2*, 49−53.
(21) Banerjee, S.; Wong, S. S. *J. Am. Chem. Soc.* **2002**, *124*, 8940−8948.
(22) Haremza, J. M.; Hahn, M. A.; Krauss, T. D. *Nano Lett.* **2002**, *2*, 1253−1258.
(23) Banerjee, S.; Wong, S. S. *Nano Lett.* **2002**, *2*, 195−200.
(24) Azamian, B. R.; Coleman, K. S.; Davis, J. J.; Hanson, N.; Green, M. L. H. *Chem. Commun.* **2002**, 366−367.
(25) Baker, S. E.; Cai, W.; Lasseter, T. L.; Weidkamp, K. P.; Hamers, R. J. *Nano Lett.* **2002**, *2*, 1413−1417.
(26) Dwyer, C.; Guthold, M.; Falvo, M.; Washburn, S.; Superfine, R.; Erie, D. *Nanotechnology* **2002**, *13*, 601−604.
(27) Shim, M.; Kam, N. W. S.; Chen, R. J.; Li, Y.; Dai, H. *Nano Lett.* **2002**, *2*, 285−288.
(28) Pompeo, F.; Resasco, D. E. *Nano Lett.* **2002**, *2*, 369−373.
(29) Huang, W.; Taylor, S.; Fu, K.; Lin, Y.; Zhang, D.; Hanks, T., W.; Rao, A. M.; Sun, Y.-P. *Nano Lett.* **2002**, *2*, 311−314.
(30) Pantarotto, D.; Partidos, C. D.; Graff, R.; Hoebeke, J.; Briand, J.-P.; Prato, M.; Bianco, A. *J. Am. Chem. Soc.* **2003**, *125*, 6160−6164.
(31) Sun, Y.-P.; Huang, W.; Lin, Y.; Fu, K.; Kitaygorodskiy, A.; Riddle, L. A.; Yu, Y. J.; Carroll, D. L. *Chem. Mater.* **2001**, *13*, 2864−2869.
(32) Sun, Y. P.; Fu, K. F.; Lin, Y.; Huang, W. J. *Acc. Chem. Res.* **2002**, *35*, 1096−1104.
(33) Mickelson, E. T.; Huffman, C. B.; Rinzler, A. G.; Smalley, R. E.; Hauge, R. H.; Margrave, J. L. *Chem. Phys. Lett.* **1998**, *296*, 188−194.
(34) Georgakilas, V.; Kordatos, K.; Prato, M.; Guldi, D. M.; Holzinger, M.; Hirsch, A. *J. Am. Chem. Soc.* **2002**, *124*, 760−761.
(35) Georgakilas, V.; Tagmatarchis, N.; Pantarotto, D.; Bianco, A.; Briand, J. P.; Prato, M. *Chem. Commun.* **2002**, 3050−3051.
(36) Bahr, J. L.; Yang, J. P.; Kosynkin, D. V.; Bronikowski, M. J.; Smalley, R. E.; Tour, J. M. *J. Am. Chem. Soc.* **2001**, *123*, 6536−6542.
(37) Holzinger, M.; Vostrowsky, O.; Hirsch, A.; Hennrich, F.; Kappes, M.; Weiss, R.; Jellen, F. *Angew. Chem., Int. Ed.* **2001**, *40*, 4002−4005.
(38) Tang, Z.; Xu, H. *Macromolecules* **1999**, *32*, 2569−2576.
(39) Curran, S. A.; Ajayan, P. M.; Blau, W. J.; Carroll, D. L.; Coleman, J. N.; Dalton, A. B.; Davey, A. P.; Drury, A.; McCarthy, B.; Maier, S.; Strevens, A. *Adv. Mater.* **1998**, *10*, 1091−1093.
(40) Star, A.; Stoddart, F. J.; Steuerman, D.; Diehl, M.; Boukai, A.; Wong, E. W.; Yang, X.; Chung, S.-W.; Choi, H.; Heath, J. R. *Angew. Chem., Int. Ed.* **2001**, *40*, 1721−1725.
(41) Star, A.; Liu, Y.; Grant, K.; Ridvan, L.; Stoddart, F. J.; Steuerman, D.; Diehl, M. R.; Boukai, A.; Heath, J. R. *Macromolecules* **2003**, *36*, 553−560.
(42) Steuerman, D. W.; Star, A.; Narizzano, R.; Choi, H.; Ries, R. S.; Nicolini, C.; Stoddart, J. F.; Heath, J. R. *J. Phys. Chem. B* **2002**, *106*, 3124−3130.
(43) Chen, J.; Liu, H. Y.; Weimer, W. A.; Halls, M. D.; Waldeck, D. H.; Walker, G. C. *J. Am. Chem. Soc.* **2002**, *124*, 9034−9035.
(44) Chen, R. J.; Zhang, Y.; Wang, D.; Dai, H. *J. Am. Chem. Soc.* **2001**, *123*, 3838−3839.
(45) Gomez, F. J.; Chen, R. J.; Wang, D. W.; Waymouth, R. M.; Dai, H. J. *Chem. Commun.* **2003**, 190−191.
(46) Nakashima, N.; Tomonari, Y.; Murakami, H. *Chem. Lett.* **2002**, 638−639.
(47) Matyjaszewski, K.; Xia, J. *Chem. Rev.* **2001**, *101*, 2921−2990.
(48) Pyun, J.; Matyjaszewski, K.; Kowalewski, T.; Savin, D.; Patterson, G.; Kickelbick, G.; Huesing, N. *J. Am. Chem. Soc.* **2001**, *123*, 9445−9446.
(49) von Werne, T.; Patten, T. E. *J. Am. Chem. Soc.* **2001**, *123*, 7497−7505.
(50) Chen, J.; Rao, A. M.; Lyuksyutov, S.; Itkis, M. E.; Hamon, M. A.; Hu, H.; Cohn, R. W.; Eklund, P. C.; Colbert, D. T.; Smalley, R. E.; Haddon, R. C. *J. Phys. Chem. B* **2001**, *105*, 2525−2528.

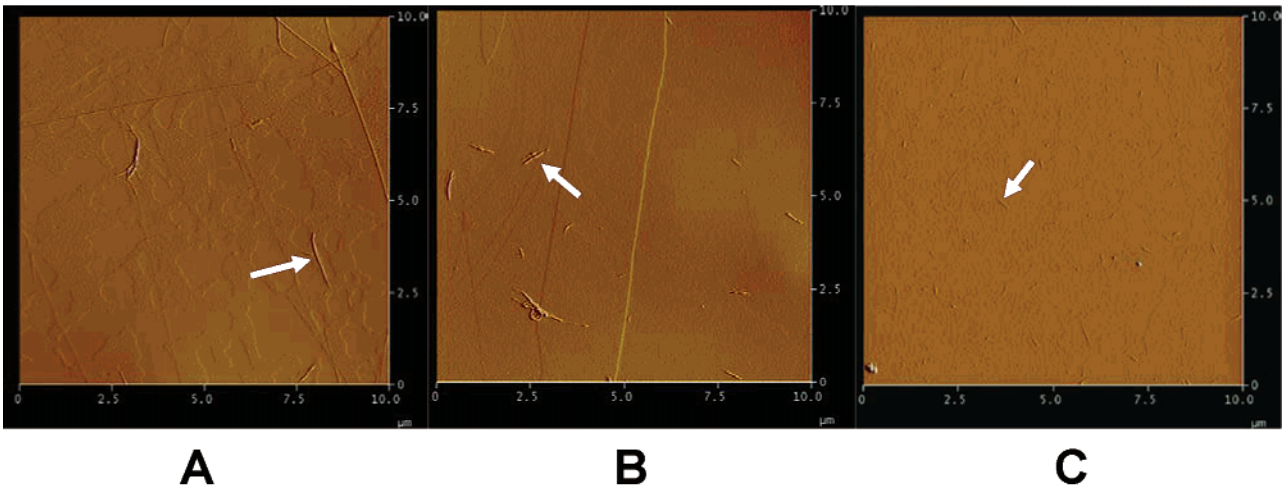

Figure 1. AFM images of the shortening process for SWNTs. (A) As-received SWNTs; (B) SWNTs after sonication for 1 h; (C) SWNTs after sonication for 2 h.

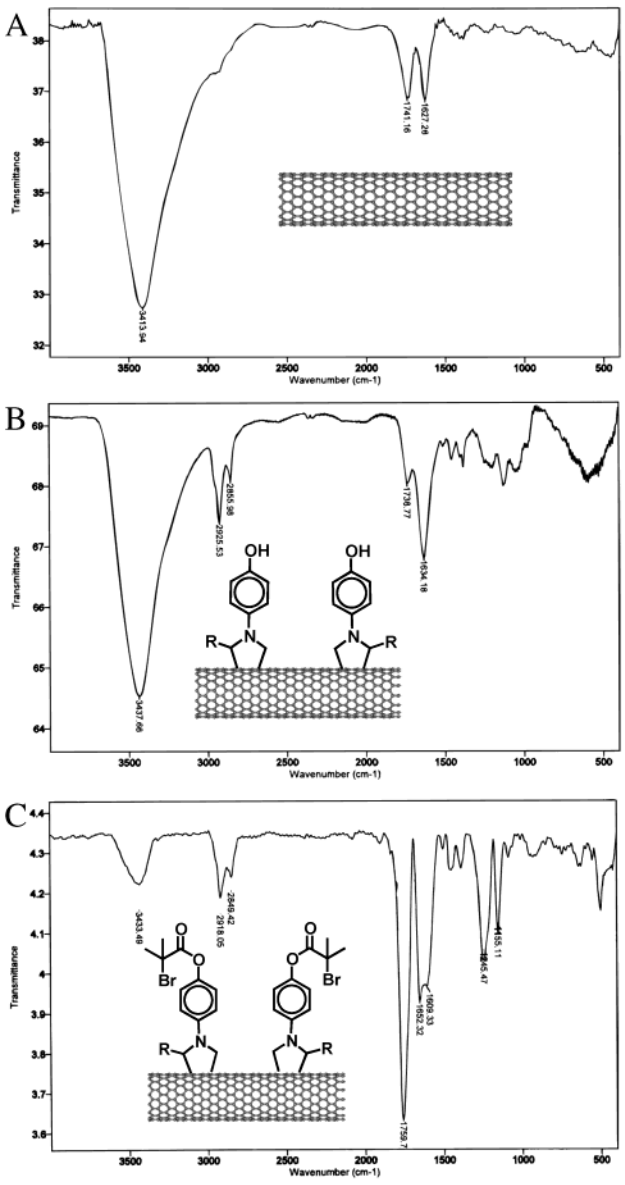

Figure 2. IR spectra for the shortened, unfunctionalized SWNTs (A), phenol-functionalized SWNTs (B), and initiator-functionalized SWNTs (C).

to the asymmetrical stretching and scissoring vibrations, respectively, due to traces of water in the KBr pellet used for the analysis. The trace water could not be removed even with extensive drying of the KBr at elevated temperatures and prolonged purging of the instrument with a stream of nitrogen gas.

Functionalization of Shortened SWNTs with ATRP Initiators. Alkyl halides, and especially alkyl bromides, can generally act as excellent atom transfer radical polymerization initiators.[47] We chose to functionalize the sidewalls of our shortened nanotubes with alkyl bromide moieties using a two-step procedure involving first a 1,3-dipolar cycloaddition[34,35] to introduce phenol functionalities, followed by an esterification with 2-bromoisobutyryl bromide (Scheme 1). Addition of 4-hydroxyphenyl glycine and octyl aldehyde to a suspension of shortened SWNTs in DMF, followed by heating at 130 °C for 5 days, resulted in the incorporation of phenol-functionalized pyrrolidine rings on the surface of the SWNTs. This was evidenced by the appearance of a clear C−H stretch at ca. 2900 cm^{-1} and the appearance of an aromatic C−C stretch at 1634 cm^{-1} in the IR spectrum (Figure 2B). The surface phenol functionalities could then be treated with 2-bromoisobutyryl bromide in DMF at 70 °C to introduce the initiating species on the sidewalls of the tubes (Scheme 1). This functionalization reaction was again followed by IR spectroscopy to monitor the appearance of C−H stretches (ca. 2900 cm^{-1}) from the alkyl portions of the attached initiators, and the appearance of a strong C═O stretch (ca. 1730 cm^{-1}) arising from the ester linkages (Figure 2C). Elemental analysis of **2** revealed the presence of both nitrogen (∼3%) and bromine (∼1%), providing further evidence that the functionalization was successful in introducing the desired alkyl bromide functionalities.

Polymerization of Methyl Methacrylate (MMA) Using SWNT Macroinitiators. Atom transfer radical polymerization (ATRP) of MMA is known to be a facile process that occurs efficiently in solution due to the relative ease of activation of the capped radical species and the favorable ATRP equilibrium constant.[47] For these reasons, we initially chose MMA for polymerization using our SWNT macroinitiators (Scheme 2). To successfully carry out this polymerization, it was necessary to choose a solvent in which the functionalized SWNTs could be well dispersed. It was also necessary to perform this reaction

Scheme 1

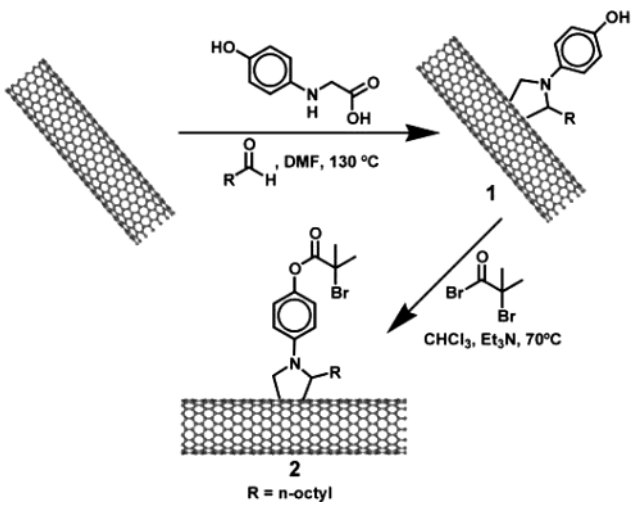

Scheme 2

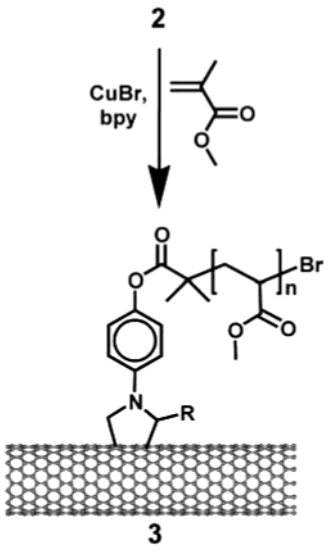

at a low temperature to minimize any spontaneous thermal polymerization and to prevent cleavage of the phenolic ester linkage between the initiating site and the nanotube. We found that an 8:3 mixture of DMF:H_2O as the solvent system allowed for adequate dispersion of the macroinitiators, and CuBr/2,2′-dipyridyl (bpy) as the catalyst/ligand combination could be used to carry out the polymerizations efficiently at room temperature.[51] In a typical polymerization, one flask was charged with 4 mg of macroinitiator (**2**), 11 mL of a DMF/H_2O mixture (8:3 v/v) as solvent, and 3 mL of MMA. This heterogeneous mixture was degassed by bubbling with a stream of N_2 for 30 min. A separate flask was charged with CuBr (40 mg) and bipyridine (175 mg) and was kept under an Ar atmosphere. Upon completion of the bubbling, the macroinitiator-containing suspension was transferred to the catalyst-containing flask via cannula, and this reaction flask was sealed. The resulting suspension was stirred at room temperature for various periods of time, ranging from 1 to 48 h. The polymerization was then worked up by dilution with THF and filtration though a 200 nm pore Teflon (Millipore) membrane. The residue was washed

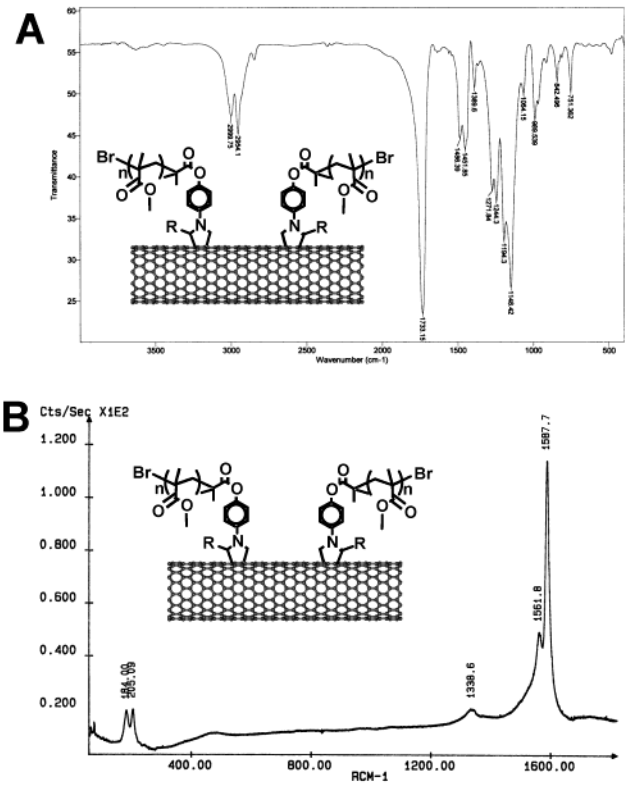

Figure 3. (A) IR spectrum of SWNT-PMMA polymerized product; (B) Raman spectrum of SWNT-PMMA polymerized product.

with THF, CH_2Cl_2, and MeOH (200 mL of each) to remove excess monomer, the catalyst complex, and any unattached polymer that may have been formed in the polymerization process. After the residue was dried under vacuum, a gray powder was isolated. This isolated product was then analyzed by IR and Raman spectroscopy, differential scanning calorimetry, as well as AFM and TEM to determine its composition.

Figure 3A illustrates the IR spectrum of a SWNT sample after 48 h of polymerization, clearly indicating the expected carbonyl stretch at ∼1730 cm^{-1} and C−H stretches at ∼2950 cm^{-1} arising from the nanotube-attached PMMA in the sample. The presence of carbon nanotubes in this residue was confirmed by Raman spectroscopy, which revealed their characteristic tangential G-band at ca. 1590 cm^{-1} and radial breathing modes at 184 and 205 cm^{-1}, corresponding to 1.2 and 1.1 nm diameter tubes, respectively.[52] The peak at 1338 cm^{-1} corresponds to the presence of a relatively small amount of sp^3-hybridized carbon atoms, formed as a result of sidewall functionalization (Figure 3B).[36,53] This combination of IR and Raman data indicates that both components are present in the sample and cannot be separated by washing with good solvents for the polymer. It should be noted that in a control experiment, where nanotubes were mixed with preformed PMMA, filtration and washing using the same protocol as outlined above resulted in complete removal of the free polymer from the nanotube residue, as indicated by the absence of IR stretches at ∼1730 and ∼2900 cm^{-1}.

Figure 4 illustrates the differential scanning calorimetry traces for bulk PMMA (Mn = 8972, PDI = 1.16) and PMMA prepared

(51) Huang, W. X.; Baker, G. L.; Bruening, M. L. *Angew. Chem., Int. Ed.* **2001**, *40*, 1510−1512.

(52) Bandow, S.; Asaka, S.; Saito, Y.; Rao, A. M.; Grigorian, L.; Richter, E.; Eklund, P. C. *Phys. Rev. Lett.* **1998**, *80*, 3779−3782.

(53) Bahr, J. L.; Tour, J. M. *Chem. Mater.* **2001**, *13*, 3823−3824.

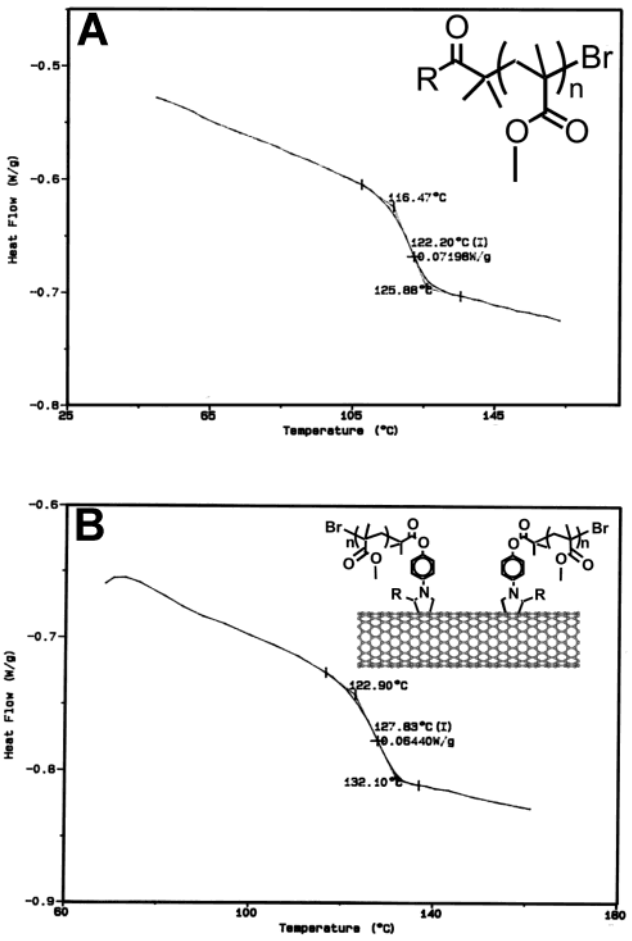

Figure 4. DSC traces for PMMA (A) and PMMA polymerized from the surface of SWNTs (B).

using the SWNT macroinitiators. It was observed that the glass transition temperature (T_g) of the polymer increased from 122 °C in the bulk to ca. 128 °C when attached to the nanotubes. It has previously been shown that constraint of polystyrene chains due to their attachment to silica surfaces results in an increase in the T_g.[54] The same phenomenon may be occurring in this case, where attachment of the polymer chains to the nanotube surface imposes constraints over their mobility, resulting in the observed 6 °C increase in T_g. In addition, polymers cleaved from the nanotubes under basic conditions (see below) were analyzed by DSC and exhibited a drop in the T_g back to 121 °C, again indicating that the elevated T_g was the result of nanotube attachment.

Further evidence for the formation of nanotube-polymer composites can be ascertained from microscopy studies. Figure 5 illustrates atomic force microscopy images of (A) initiator-functionalized and (B) polymer-functionalized (48 h polymerization) SWNTs. The measured height profiles of representative initiator-functionalized tubes ((i) and (ii) in Figure 5A) revealed that they were bundles, ranging in height between 5 and 15 nm. This indicates that sidewall functionalization of the tubes with relatively small structures does not lead to the dissociation of nanotube bundles. Upon polymerization of MMA, it is clear that large, globular structures became associated with the carbon nanotubes. It is postulated that these structures correspond to nanotube-attached PMMA. The height profiles of the larger globular structures indicate heights ranging from 20 to 40 nm. Smaller polymer-associated nanotube structures can also be observed. Interestingly, in Figure 5B (box), a portion of a single SWNT can be seen spanning the distance between two polymerized areas, indicating that either initiator functionalization is not homogeneously spread over the entire length of the SWNTs or that some initiator sites are not active during the polymerization. Additionally, the height of this nanotube structure was measured to be on the order of 0.9 nm, indicating that it is a single tube, rather than a bundle of tubes. It is possible that, during polymerization, at least some of the SWNTs initially present in bundles are separated into individual tubes, presum-

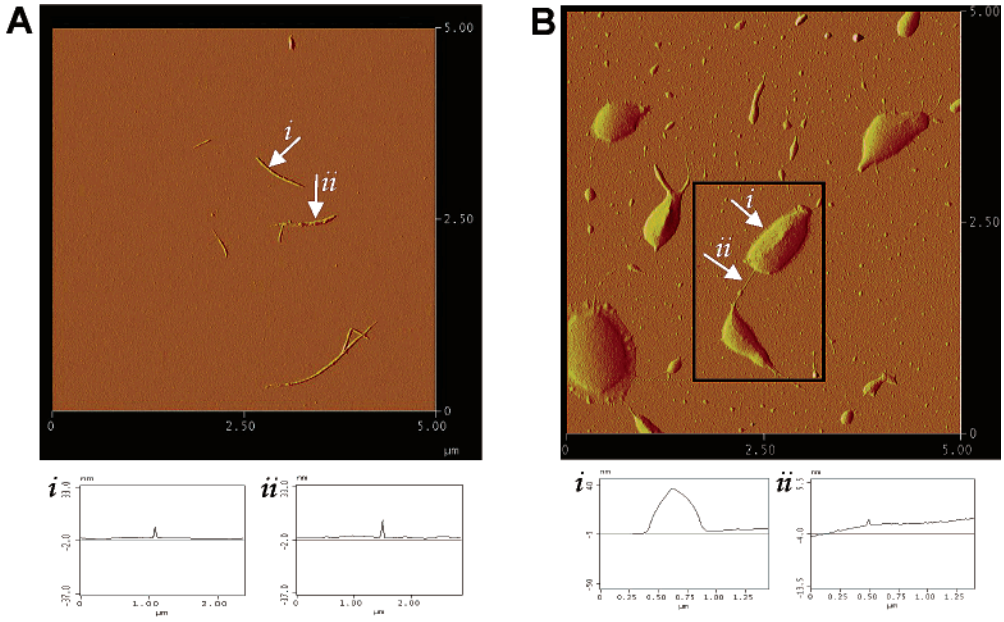

Figure 5. AFM images and height profiles of initiator-functionalized carbon nanotubes before (A) and after (B) polymerization of MMA. Arrows indicate the location at which the cross-sectional height profiles were obtained. The polymerized sample was obtained after a 48 h polymerization time. In (B), the box surrounds a feature in which a single SWNT spans the distance between two areas of polymer.

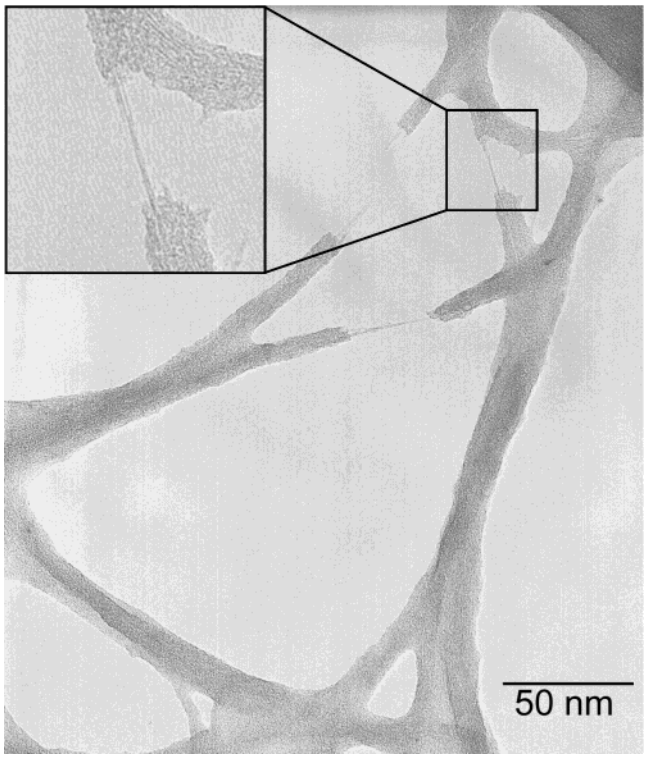

Figure 6. TEM micrograph of SWNT-PMMA conjugate. Inset shows a close-up view of a nanotube-bridged gap in the polymer structure.

ably due to steric repulsion caused by the growing polymer chains.

Polymer coated SWNTs were also observed by transmission electron microscopy (TEM). Samples were prepared by dispersing suspensions of the polymerized nanotubes onto a holey carbon-coated copper grid. These samples produced a film in which it was possible to discern embedded SWNTs. Upon irradiation with the electron beam, the polymer film was observed to craze and dewet such that it became closely associated with the nanotube skeleton to produce structures in which individual nanotubes and small nanotube bundles are sheathed by regions of amorphous carbon, presumably corresponding to the polymer portion of the sample (Figure 6). In some areas, these sheathed structures were found to contain gaps that were bridged by SWNTs (Figure 6, inset). The structures produced after the dewetting process were more stable to the electron beam than the original polymer film, indicating that the SWNT skeleton reinforces the overall composite structure. Figure 6 again provides some evidence that larger nanotube bundles are separated into smaller bundles or even individual tubes through the polymerization process, likely as a result of steric repulsion between growing polymer chains.

To gain insight into whether the nanotube-initiated MMA polymerization process is a controlled/living polymerization, a study was performed in which the sample mass increase and the polymer molecular weight were correlated to the polymerization time. The mass increase of the samples after a specific polymerization interval was measured gravimetrically after filtration, washing with excess solvent, and thorough drying of the samples in vacuo. The molecular weight of the polymers was measured by GPC after cleaving the phenolic ester bond

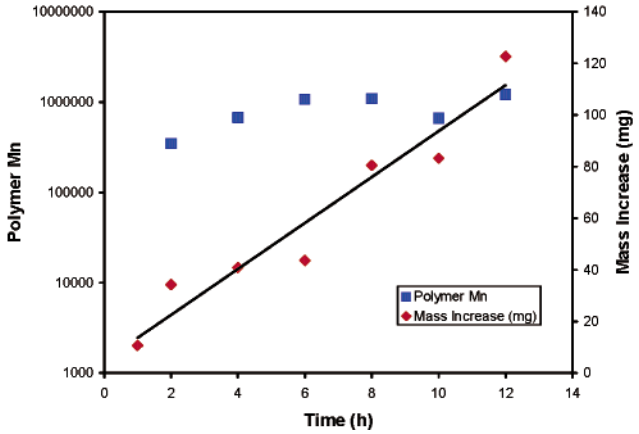

Figure 7. Evolution of the mass increase of the nanotube-PMMA composites and polymer molecular weight as a function of polymerization time.

that links the initiator to the nanotube using excess $NaHCO_3$ in a mixture of $MeOH/CH_2Cl_2$ (2:7 v/v).[55] After cleavage, the polymer was isolated by first diluting the reaction mixture with THF and then passing the solution through a plug of silica gel with THF as the eluent. Any SWNTs present in the sample were easily removed by this procedure, allowing the isolation of pure polymer samples. It was found that the mass of the nanotube sample increased with time in a nearly linear fashion, but the polymer molecular weight did not follow this trend (Figure 7). In fact, extremely high molecular weights, in excess of 300 000 g/mol, were observed even after relatively short polymerization times (2 h). In addition, the polydispersity index (PDI) of the recovered polymer chains was consistently greater than 1.6. These results indicate that, as the polymerization time lengthens, the elevation in sample mass results from an increased number of nanotube-bound initiators promoting rapid, uncontrolled growth of polymer chains, rather than any controlled polymer molecular weight increase over time. Furthermore, all attempts to chain-extend the grafted polymers did not result in any significant mass enhancement, again indicating that the polymerizations were not living and had terminated irreversibly. It is possible to utilize the measured polymer molecular weight data, along with the sample mass increase, to make an initial, very crude estimate of the average number of polymer chains that are attached to an individual SWNT. Using an approximate nanotube molecular weight of 668 000 g/mol[56] and an initial sample mass of 4 mg, we estimated that the number of attached polymer chains varies between 7 and 21 per nanotube, depending on the sample (see Supporting Information).

A recent report has shown that ATRP using surface-bound initiators results in uncontrolled, very rapid polymerization due to an extremely low concentration of the deactivating $CuBr_2$ species in solution.[57] It was demonstrated that addition of either sacrificial initiator or the $CuBr_2$ deactivator to the reaction mixture resulted in recovery of control over the polymerization from silicon substrates.[57,58] We postulated that similar approaches might help to control the SWNT-initiated polymeriza-

(54) Savin, D. A.; Pyun, J.; Patterson, G. D.; Kowalewski, T.; Matyjaszewski, K. *J. Polym. Sci., Part B: Polym. Phys.* **2002**, *40*, 2667−2676.

(55) Shashidhar, M. S.; Bhatt, M. V. *J. Chem. Soc., Chem. Commun.* **1987**, 654−656.

(56) Hamon, M. A.; Chen, J.; Hu, H.; Chen, Y. S.; Itkis, M. E.; Rao, A. M.; Eklund, P. C.; Haddon, R. C. *Adv. Mater.* **1999**, *11*, 834−840.

(57) Matyjaszewski, K.; Miller, P. J.; Shukla, N.; Immaraporn, B.; Gelman, A.; Luokala, B. B.; Siclovan, T. M.; Kickelbick, G.; Vallant, T.; Hoffmann, H.; Pakula, T. *Macromolecules* **1999**, *32*, 8716−8724.

tions and produce narrow polydispersity chains attached to the nanotubes. However, our attempts to add sacrificial initiators to the nanotube-initiated polymerizations resulted in the exclusive formation of free polymer in solution, with no observable mass increase in the recovered nanotube samples. Clearly, the extremely low number of nanotube-attached initiating sites could not compete with the unattached initiators in the reaction mixture. Additionally, control experiments in which ATRP using unbound initiators was carried out in the presence of unfunctionalized SWNTs, under conditions identical to those of our SWNT-initiated polymerizations, resulted in the production of free polymers having broad polydispersities (PDI $>$ 2.5) and higher than expected molecular weights. This indicates that it may be the presence of the nanotubes that prevents the polymerization from being a "living" process. It should be noted that solution polymerizations in the absence of SWNTs, using the same conditions as above, consistently yielded well-defined polymers having the expected molecular weights and narrow polydispersities (PDI $<$ 1.2). Addition of $CuBr_2$ rather than sacrificial initiator to these experiments similarly did not result in any improved "living" character, again resulting in polymers having broad polydispersities (PDI $\approx$ 3.45). These results indicate that the presence of carbon nanotubes causes a decrease in the concentration of the persistent radicals in solution,[59] thereby decreasing the degree of control over the polymerization process. Recently, it has been shown that radical species produced when benzoyl peroxide is decomposed in the presence of alkyl iodides can be used to functionalize the sidewalls of carbon nanotubes.[60] In these reactions, the nanotubes act as radical scavengers, thereby removing radical species from solution. We believe that similar reactions may be occurring in our experiments, resulting in the elimination of the radical capping agents that are necessary for control of the polymerization process.

Solubility of Polymerized SWNTs. Considering our initial goal of improving nanotube solubility and processability, we investigated the solubility of the polymerized SWNTs in various organic solvents. We were disappointed to find that the PMMA chains attached in our initial experiments did not impart any enhanced solubility to the nanocomposites in CH_2Cl_2, $CHCl_3$, THF, acetone, or even DMF and DMSO. When the high solubility of PMMA in organic solvents such as THF was considered, it was surprising that no solubility enhancement was observed for these samples. One possible explanation for the poor solubility of the nanocomposites is the potential for cross-linking to occur during polymerization as a result of radical coupling of the growing polymer chain ends. Such cross-linking can occur between chain ends of polymers growing from a single nanotube, or between polymers growing from different SWNTs, possibly within a nanotube bundle. The former case would prevent polymers from extending into solution, decreasing their solubility. In the latter case, large networks of nanotubes interconnected by polymer chains could be formed and would be too large to allow for effective solubilization. Although these structures were not soluble, TEM comparison of the polymerized nanotubes to control experiments in which the initiators were not bound to the nanotubes clearly demonstrated a significant difference in nanotube dispersion (Figure 8). In the control experiments, the nanotube distribution was not nearly as homogeneous as it was in the samples where polymers were covalently attached to the nanotubes. The control experiments exhibited many regions containing only clusters of carbon nanotubes with very little associated polymer, whereas the covalently functionalized nanotubes were very evenly distributed throughout the sample. This is consistent with the previously observed phase separation of nanotubes from bulk polymers in simple mixtures of the two materials.[61] This phase separation is caused by the substantial van der Waals interactions that occur between nanotubes and precludes the homogeneous dispersion of unfunctionalized nanotubes in bulk polymers.

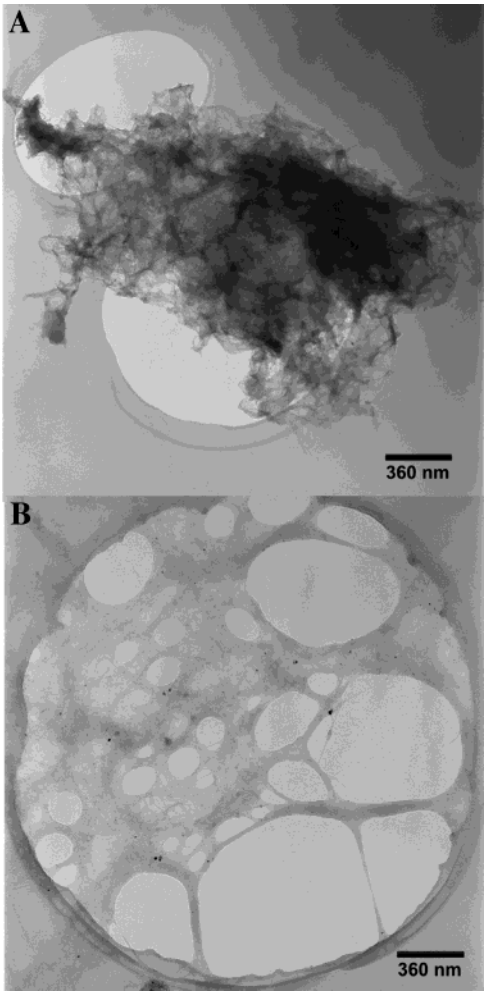

Figure 8. Transmission electron micrographs of (A) a sample of SWNTs mixed with PMMA and (B) a sample of polymerized SWNTs. In the former case, agglomeration of carbon nanotubes is clearly visible with very little associated polymer. In the latter case, carbon nanotubes are embedded within polymer regions in a much more uniform manner.

To further explore the possibility of solubilizing SWNTs, we chose to investigate the polymerization of *tert*-butyl acrylate (*t*BuA). We postulated that the bulkier *tert*-butyl group on each monomer unit might enhance the solubility of the polymerized tubes and possibly decrease the chance of cross-linking by radical coupling. In addition, it is well known that removal of

(58) Husseman, M.; Malmstrom, E. E.; McNamara, M.; Mate, M.; Mecerreyes, D.; Benoit, D. G.; Hedrick, J. L.; Mansky, P.; Huang, E.; Russell, T. P.; Hawker, C. J. *Macromolecules* **1999**, *32*, 1424−1431.
(59) Fischer, H. *Macromolecules* **1997**, *30*, 5666−5672.
(60) Ying, Y. M.; Saini, R. K.; Liang, F.; Sadana, A. K.; Billups, W. E. *Org. Lett.* **2003**, *5*, 1471−1473.
(61) Park, C.; Ounaies, Z.; Watson, K. A.; Crooks, R. E.; Smith, J.; Lowther, S. E.; Connell, J. W.; Siochi, E. J.; Harrison, J. S.; Clair, T. L. S. *Chem. Phys. Lett.* **2002**, *364*, 303−308.

Scheme 3

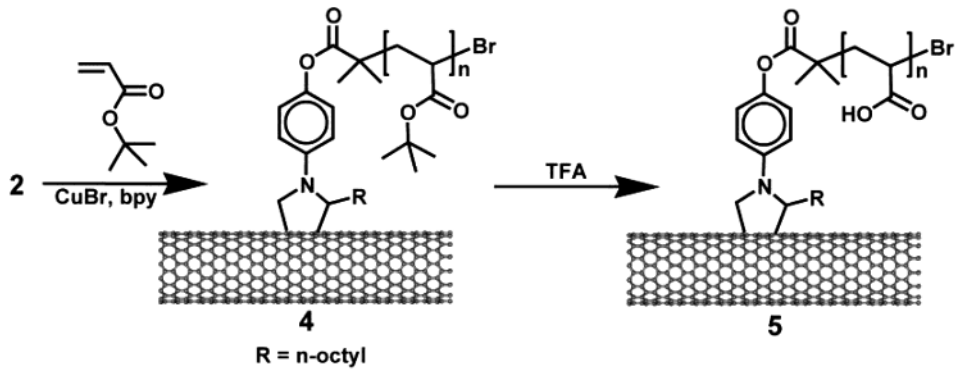

the *tert*-butyl groups can be efficiently performed under acidic conditions, leading to the formation of poly(acrylic acid), which is soluble in aqueous solutions. The prospect of modulating the solubility of the nanocomposites through postpolymerization chemistry was appealing and was a motivating factor for switching to this particular monomer.

The SWNT macroinitiator **2** was used to polymerize *t*BuA under conditions identical to those of the polymerization of MMA (Scheme 3). After polymerization, the SWNT nanocomposites were isolated using procedures identical to those used for the PMMA-functionalized nanotubes. The IR and Raman spectra for this sample are given in Figure 9. Characteristic IR stretches at ca. 1730 cm^{-1} and ca. 2950 cm^{-1} indicate the presence of polymer, while Raman signals at ca. 185 and 1590 cm^{-1} correspond to the radial breathing modes and the tangential modes of the SWNT. It is not entirely clear why the radial breathing mode in this sample corresponds solely to nanotubes having a diameter of 1.2 nm, but this is likely due to heterogeneity of different batches of starting material. In addition, a significant disorder peak at 1338 cm^{-1} is apparent, corresponding to the presence of sp^3-hybridized carbon atoms within the nanotubes formed as a result of the functionalization process. This disorder peak is proportional to the extent of nanotube functionalization. DSC performed on this sample indicated a T_g of 46.6 °C, which is slightly higher than the T_g of poly(*tert*-butyl acrylate), observed at 43.1 °C.

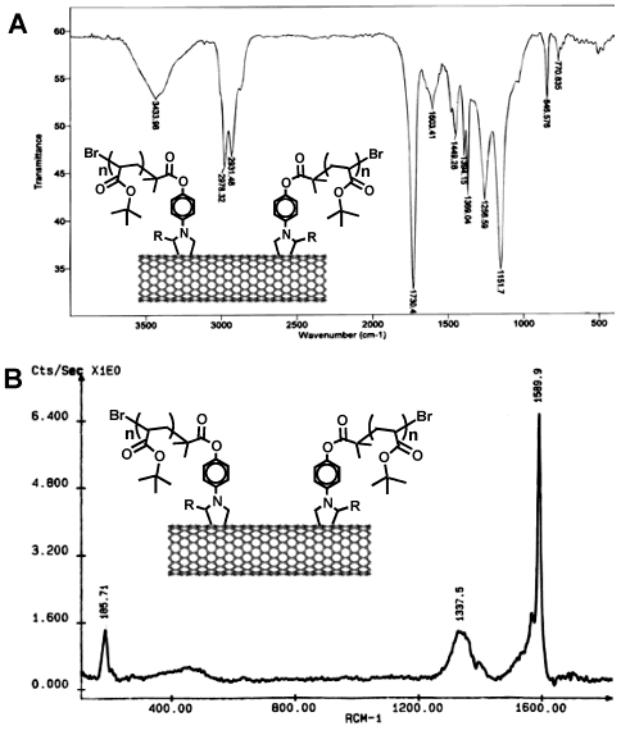

Figure 9. Analysis of poly(*tert*-butyl acrylate)-functionalized SWNTs using (A) FT-IR and (B) Raman spectroscopy.

The poly(*tert*-butyl acrylate)-functionalized nanotubes (**4**) were found to be soluble in a range of organic solvents, including CH_2Cl_2, $CHCl_3$, and THF (Figure 10). Using UV/vis absorption spectroscopy at 500 nm and the reported specific extinction coefficient of $\epsilon_{500} = 28.6$ cm^2/mg,[62] the estimated nanotube concentration in the THF solution was 50.3 mg/L. Solution NMR spectroscopy also provided evidence that the polymer is present within this material (Figure 11). Aliphatic proton signals were observed in the region between 0.8 and 1.8 ppm, corresponding to the polymer backbone protons as well as the *tert*-butyl side chains. No signals corresponding to the aromatic protons of the phenol linker between the pyrrolidine ring and the polymer were observed due to the extremely low concentration and mobility of these groups within the structures.

The solubility of the poly(*tert*-butyl acrylate)-functionalized nanotubes could be drastically affected by removal of the *tert*-butyl groups. This was accomplished by stirring the nanotubes in a 10% trifluoroacetic acid (TFA)/CH_2Cl_2 solution (v/v) for 12 h (Scheme 3). Upon evaporation of the solvent and acid, the resulting PAA-functionalized nanotubes (**5**) were found to be soluble in a 10 mM NaOH solution (Figure 10C) and

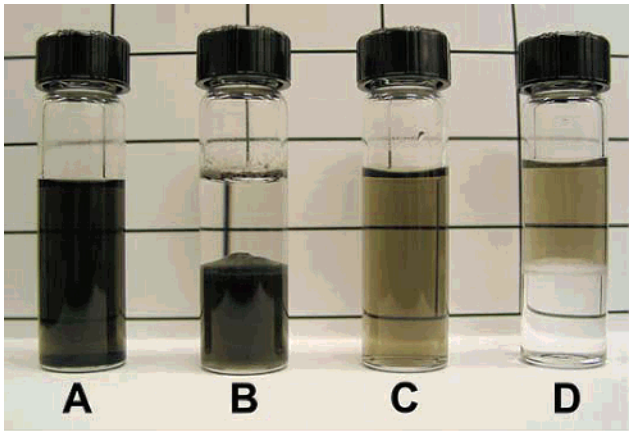

Figure 10. Solutions of polymerized nanotubes. (A) Poly(*tert*-butyl acrylate)-nanotube sample in THF; (B) poly(*tert*-butyl acrylate)-nanotube sample in a mixture of H_2O/CH_2Cl_2; (C) poly(acrylic acid)-nanotube sample in H_2O; (D) poly(acrylic acid)-nanotube sample in a mixture of H_2O/CH_2Cl_2.

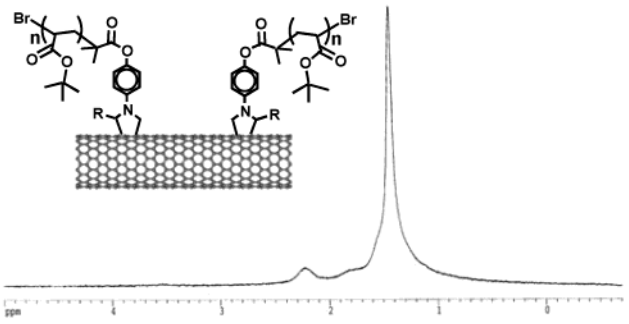

Figure 11. ^{1}H NMR spectrum of poly(*tert*-butyl acrylate)-functionalized SWNTs in $CDCl_3$.

completely insoluble in organic solvents such as CH_2Cl_2. UV/vis measurements were again used to estimate the nanotube concentration, which was found to be approximately 19.7 mg/L in this solution. Furthermore, the solution remained stable for several weeks, with no apparent precipitation of the polymerized SWNTs.

Conclusions

The 1,3-dipolar cycloaddition reaction on the surface of SWNTs using octanal and 4-hydroxyphenyl glycine resulted in phenol-functionalized tubes that could be further derivatized with 2-bromoisobutyryl bromide. The resulting modified SWNTs served as ATRP initiators for MMA and *t*BuA, allowing for the formation of SWNT-polymer nanocomposites. IR, Raman, and DSC analysis indicated that both nanotubes and polymers were present within the material isolated from the polymerization reaction. Unlike simple blends of polymers and nanotubes, the two components of our composites could not be separated from one another by extensive filtration and washing, indicating that they are covalently bound. Analysis of these structures by AFM and TEM provided further evidence for the formation of polymerized nanotubes and indicated that, in some instances, large nanotube bundles could be dissociated by the growth of polymers from their surface. Further, it was found that the attached polymers could be cleaved from the nanotubes. SEC analysis of the cleaved polymers demonstrated that the surface polymerizations were not controlled and resulted in extremely high molecular weight and PDI values. Attempts to add sacrificial initiators or $CuBr_2$ to the polymerizations were unsuccessful in improving control. Although the PMMA-functionalized tubes were not soluble in organic solvents, the poly(*tert*-butyl acrylate)-functionalized tubes did exhibit good solubility in organic solvents such as CH_2Cl_2, $CHCl_3$, and THF. Upon removal of the *tert*-butyl groups, the resulting PAA-functionalized tubes became soluble in aqueous solvents.

Experimental Section

General. Single-walled carbon nanotubes (SWNTs) were purchased from Carbon Nanotechnologies, Inc. (Houston, TX). *N*-(4-Hydroxyphenyl) glycine was purified by recrystallization from distilled H_2O. Methyl methacrylate (MMA) and *tert*-butyl acrylate (*t*BA) were purified by passing through basic alumina and were stored in the refrigerator. All other reagents and solvents were purchased from commercial suppliers and used as received. FTIR was performed on a Bio-Rad FTS-40 instrument. All samples were prepared as pellets using spectroscopic grade KBr in a Carver press at 15 000 psi. Laser Raman spectroscopy was performed on a Jobin-Yvon SR-3000 macro/micro-Raman spectrometer operating with a 514.5 nm Ar ion laser (Spectra Physics). Atomic force microscopy was done using a Digital Instruments NanoScope IIIa Multimode AFM, with samples prepared by drop casting sample solutions or suspensions on either HOPG or freshly cleaved mica substrates. The images were recorded with standard tips in tapping mode at a scan rate of 1.0 Hz. TEM analysis was performed using a Philips CM12 operating at 120 keV. NMR was performed on a Bruker 200 MHz instrument in $CDCl_3$. Differential scanning calorimetry (DSC) was performed on a TA 2100 modulated differential scanning calorimeter with a temperature gradient of 15 deg/min. Ultrasonication was done in a Banson Ultrasonics B1510 bath sonicator. Filtration was done through either a 100 nm-pore polycarbonate membrane (Millipore) or a 200 nm-pore Teflon membrane (Millipore). Polymer molecular weight and polydispersity index (PDI) were estimated by gel permeation chromatography (GPC) using a Waters 2695 Separations Module equipped with a Waters 2996 photodiode array detector, a Waters 2414 refractive index detector, a Waters 2475 Multi λ fluorescence detector, and four Polymer Labs PLgel individual pore size columns. Polystyrene standards were used for calibration, and tetrahydrofuran (THF) was used as the eluent at a flow rate of 1.0 mL/min. The concentrations of the soluble polymer-functionalized SWNTs were calculated from UV/vis absorption spectra measured using a Cary 50 UV−visible spectrophotometer.

Shortening and Purification of SWNTs. A 250 mL flask charged with 50 mg of SWNTs and 100 mL of a H_2SO_4/HNO_3 (v/v 3/1) solution was sonicated for 2 h. The mixture was then diluted with 200 mL of distilled water. After being cooled to room temperature, the diluted solution was filtered through a 100 nm-pore polycarbonate membrane. The black material collected from the membrane was further treated by stirring with 50 mL of H_2SO_4/H_2O_2 (9/1) in a 250 mL flask for 30 min at room temperature. Another 50 mL of H_2SO_4/H_2O_2 (9/1) was added, and the solution was sonicated for 5 min. After dilution using 200 mL of distilled water, the solution was filtered through a 100 nm-pore polycarbonate membrane. The resulting mat of SWNTs was washed thoroughly using first a 10 mM NaOH solution, and then distilled water until the pH of the filtrate was 7. The purified SWNTs were then dried under vacuum overnight. IR (KBr pellet): 1741 (s), 1627 (m) cm^{-1}.

Synthesis of Macroinitiator (2). Step 1: Purified SWNTs (30 mg), octyl aldehyde (2 mL, 0.012 mol), and *N*-(4-hydroxyphenyl) glycine (50 mg, 3.0×10^{-4} mol) were dispersed in 50 mL of DMF in a 250 mL round-bottom flask. The mixture was stirred at 130 °C under argon for 5 days with further addition of 50 mg (3.0×10^{-4} mol) aliquots of *N*-(4-hydroxyphenyl) glycine once every 24 h. At the end of this process, the product was collected by filtration through a 200 nm-pore Teflon membrane and was then washed thoroughly with CH_2Cl_2 (100 mL), THF (50 mL), and methanol (50 mL), and finally dried under vacuum overnight. IR (KBr pellet): 3437 (s), 2926−2855 (m), 1634 (s) cm^{-1}.

Step 2: A 50 mL flask was charged with anhydrous DMF (20 mL), phenol-functionalized SWNTs (20 mg), 2-bromoisobutyryl bromide (1 mL, 8 mmol), and triethylamine (1 mL, 7 mmol). The mixture was stirred at 70 °C under argon for 48 h. The product was isolated by filtration through a 200 nm-pore Teflon membrane and thoroughly washed with CH_2Cl_2 (100 mL), THF (50 mL), and methanol (50 mL), and then dried under vacuum overnight. IR (KBr pellet): 2918−2849 (m), 1759 (s), 1652−1609 (m) cm^{-1}. Elemental analysis: C, 67.10; H, 4.33; N, 2.99; Br, 0.90.

Synthesis of Poly(methyl methacrylate)-Functionalized Nanotubes (3). Four milligrams of SWNT macroinitiator (**2**) was dispersed in 8 mL of DMF, 3 mL of deionized H_2O, and 3 mL (28 mmol) of MMA in a 25 mL flask. The mixture was degassed by bubbling with N_2 for 30 min and was then transferred using a cannula to another 25 mL flask charged with 2,2′-dipyridyl (175 mg, 1.12 mmol) and CuBr (40 mg, 0.28 mmol) under argon. The polymerization was carried out

(62) Bahr, J. L.; Mickelson, E. T.; Bronikowski, M. J.; Smalley, R. E.; Tour, J. M. *Chem. Commun.* **2001**, 193−194.

at room temperature for 24 h. The polymer-functionalized SWNTs were purified by washing with THF, CH_2Cl_2, and methanol (200 mL of each) successively during filtration through a 200 nm-pore Teflon membrane. The isolated gray product from the membrane was dried under vacuum overnight. IR (KBr pellet): 2999−2954 (m), 1733 cm^{-1} (s).

Synthesis of Poly(*tert*-butyl acrylate)-Functionalized Nanotubes (4). Polymerization of *tert*-butyl acrylate was accomplished under the same conditions as those used for the polymerization of MMA. Upon precipitation, centrifugation (5000 rpm, 10 min) was used instead of filtration to isolate the product due to its tackiness. Suspensions of the product in THF were centrifuged three times, decanting the supernatant after each centrifugation cycle to remove any free polymer that may have formed in the reaction. The resulting black film (residue) was dried under vacuum overnight. ^{1}H NMR (200 MHz, $CDCl_3$): δ 2.23 (broad), 1.70 (broad), and 1.43 (broad) ppm. IR (KBr pellet): 2978−2931 (m), 1730 cm^{-1} (s).

Synthesis of Poly(acrylic acid)-Functionalized SWNTs (5). Poly (*tert*-butyl acrylate) (P*t*BA)-functionalized SWNTs (10 mg) were deprotected by stirring in a mixture of trifluoroacetic acid (TFA) (1 mL) and anhydrous CH_2Cl_2 (10 mL) at room temperature under argon for 12 h. The product was isolated by flowing nitrogen gently into the flask to remove the TFA and CH_2Cl_2, followed by drying under vacuum overnight. IR (KBr pellet): 2924−2854 (m), 1717 cm^{-1} (s).

Cleavage of Poly(methyl methacrylate) from the SWNTs. In a typical cleavage experiment, 30 mg of PMMA-functionalized SWNTs was mixed with 7 mL of CH_2Cl_2 in a 25 mL flask, followed by the addition of 2 mL of a saturated solution of $NaHCO_3$ in methanol, and a further 100 mg of $NaHCO_3$. The mixture was stirred overnight at room temperature. The cleaved polymer was isolated by filtering through a 200 nm-pore Teflon membrane and thoroughly washing the residue with THF. The filtrate was concentrated in vacuo, and the cleaved polymer was isolated by precipitation into 20 mL of MeOH. After filtration, the product was dried under vacuum overnight. ^{1}H NMR (200 MHz, $CDCl_3$): δ 3.59, δ 1.81−1.87, δ 0.84−1.02 ppm.

Typical Polymerization of Acrylate Monomers in Solution. A 25 mL flask was charged with 8 mL of DMF, 3 mL of deionized H_2O, and 3 mL (28 mmol) of MMA, and the resulting mixture was degassed by bubbling with N_2 for 30 min. This degassed solution was transferred using a cannula to another 25 mL flask charged with 175 mg of 2,2′-dipyridyl (1.12 mmol) and 40 mg of CuBr (0.28 mmol) under argon. The polymerization was carried out at room temperature for 24 h. The product was precipitated into 200 mL of MeOH and, after filtration, was dried under vacuum overnight (yield, 85%).

Acknowledgment. Financial support for this work was provided by the Natural Science and Engineering Research Council of Canada (NSERC), McMaster University, and Materials and Manufacturing of Ontario (Emerging Materials Knowledge Fund). We would like to thank Andy Duft for help with AFM as well as Profs. Mitchell Winnik and Mark Parnis for helpful suggestions and discussions.

Supporting Information Available: Raman data for unfunctionalized nanotubes as well as a table listing measured polymer molecular weights and an estimated number of polymer chains per nanotube (PDF). This material is available free of charge via the Internet at http://pubs.acs.org.

JA037564Y